Food & Function

ROYAL SOCIETY OF CHEMISTRY

PAPER

View Article Online
View Journal | View Issue

Cite this: *Food Funct.*, 2021, **12**, 10023

The petroleum ether extract of *Brassica rapa* L. induces apoptosis of lung adenocarcinoma cells *via* the mitochondria-dependent pathway†

Xierenguli Halike,‡[a] Jinyu Li,‡[b] Pengfei Yuan,[a] Kaimeiliya Yasheng,[a] Min Chen,[a] Lijie Xia *[a] and Jinyao Li*[a]

Brassica rapa L. is one of the most popular traditional foods with a variety of biological activities. In this study, the petroleum ether extract of *B. rapa* was separated by silica gel column chromatography, and named BRPS, which was identified by LC-MS. The effects and pharmacological mechanisms of BRPS on the treatment of lung cancer were investigated both *in vitro* and *in vivo*. The results showed that BRPS significantly inhibited the proliferation of both human lung cancer A549 and mouse lung cancer LLC cells, while its toxicity to normal cells was lower than that of cancer cells. BRPS induced cell cycle arrest at the G2/M phase and significantly reduced the levels of CDK1 and CyclinB1 in A549 cells. Moreover, BRPS induced apoptosis in a dose-dependent manner, and increased the Bax/Bcl-2 ratio, while it decreased mitochondrial membrane potential, promoted the release of cytochrome c, activated caspase 9 and 3, and enhanced the degradation of PARP in A549 cells. Furthermore, the levels of reactive oxygen species (ROS) were also upregulated by BRPS and ROS inhibitor reversed BRPS-induced apoptosis. Importantly, BRPS significantly suppressed the growth of LLC cells *in vivo* without any obvious side effect on body weight and organs of mice, and increased the proportion of B cells, $CD4^+$ T cells, $CD8^+$ T cells and $CD44^+CD8^+$ T cells in the spleen. These results revealed that BRPS inhibited the growth of lung cancer cells through inducing cell cycle arrest, mitochondria-dependent apoptosis, and activating immunity of mice, and BRPS might be a potential antitumor functional food and promising agent for the treatment of lung cancer.

Received 18th May 2021,
Accepted 8th August 2021

DOI: 10.1039/d1fo01547h

rsc.li/food-function

1 Introduction

Globally, lung cancer is the most common cause of cancer-related death for both men and women, with an estimated 2.2 million new cancer cases and 1.8 million deaths in 2020, accounting for 18.0% of all cancer deaths. In most countries, the survival rate for patients with lung cancer within five years after diagnosis is only 10% to 20%.[1] Environmental exposure including air pollution, radiation, asbestos and other substance exposure is the main cause of lung cancer, especially tobacco exposure, which is the most important environmental factor.[2,3] In addition, genetic factors also play an important role in the occurrence and development of lung cancer. Although the diagnosis and treatment strategies of lung cancer have made great progress in recent years, lung cancer is still one of the malignant tumors with poor prognosis due to its complicated etiology and unknown pathogenesis.[4,5]

The treatment of lung cancer mainly includes surgery, chemotherapy, radiotherapy, immunotherapy or their combination, depending on the type of cancer, the degree of cancer progression and the general health status of the patient. The cancer is usually removed surgically at the early stage.[6] However, radiotherapy might serve as a more appropriate option rather than surgery if the health condition is not optimistic.[7] Recently, targeted therapy has been playing an increasingly important role in advanced lung cancer because the signaling transduction pathway plays a crucial role in the occurrence and development of lung cancer. The main obstacle of lung cancer targeted therapy and chemotherapy is drug resistance.[8,9] The effect of traditional Chinese medicine (TCM) is often the result of multi-component and multi-target action, which has played an important role in anticancer therapy. TCM has more abundant structures and biological activities than conventional drugs, and has become a huge source for the development of anticancer drugs.[10]

Brassica rapa L. is a biennial herb of the Brassica genus in Cruciferae and widely distributes in Xinjiang, China, and can

[a]*Xinjiang Key Laboratory of Biological Resources and Genetic Engineering, College of Life Science and Technology, Xinjiang University, Urumqi, Xinjiang, China. E-mail: ljyxju@xju.edu.cn, xialijie1219@163.com*
[b]*College of Life Science, Xinjiang Normal University, Urumqi, Xinjiang, China*
†Electronic supplementary information (ESI) available. See DOI: 10.1039/d1fo01547h
‡These authors contributed equally.

be used as both food and medicine.[11] Multiple bioactive components in *B. rapa*, such as glucosinolates, isothiocyanate, phenolic compounds, flavonoids, organic acids, and polysaccharides were identified.[12–14] The bioactivity studies on *B. rapa* revealed its anticancer, immunomodulatory, anti-hypoxia and anti-oxidation activity.[15–18] Our previous study found that the *n*-butanol subfraction of *B. rapa* showed potential anti-lung cancer activity.[19] The study about anti-tumor activity proves that *B. rapa* polysaccharides have anti-lung cancer activity and induce apoptosis in A549 cells through mitochondria-mediated apoptosis.[11] Although *B. rapa* is a very important crop with edible and medicinal values, only a few studies consistently characterize its chemical characteristics and biological activities.

In this study, the petroleum ether extract of *B. rapa* was prepared and separated by silica gel chromatography, which was named BRPS. The antitumor effect and underlying mechanism of BRPS on lung cancer were investigated both *in vitro* and *in vivo*. We found that BRPS significantly inhibited the proliferation of lung cancer cells, and induced cell cycle arrest and apoptosis by activating the mitochondria-mediated apoptosis pathway *in vitro*. Moreover, BRPS significantly suppressed the growth of LLC cells *in vivo*. In addition, BRPS showed an immunostimulatory effect without obvious toxicity in mice. These results suggested that BRPS might be a potential anti-tumor functional food and agent in the treatment of lung cancer.

2 Materials and methods

2.1 Cell lines and cell culture

The human lung adenocarcinoma cell A549, normal bronchial epithelium cell BEAS-2B and murine lung carcinoma LLC cells were obtained from iCell Bioscience Inc (Shanghai, China) and cultured in DMEM medium (Gibco) supplemented with 10% heat-inactivated fetal bovine serum (MRC), 100 U ml^{-1} penicillin and 100 μg mL^{-1} streptomycin at 37 °C in a humidified atmosphere of 5% CO_2.

2.2 Isolation of active components of *B. rapa*

B. rapa was collected from Urumqi in Xinjiang, China. The dry powder of *B. rapa* was dissolved in petroleum ether at a ratio of 1 : 10, and ultrasonicated at 50 °C for 20 min, then extracted at 60 °C for 2 h. The supernatant was collected and condensed by rotary evaporation, then dried at room temperature (RT). The dry extract was dissolved in petroleum ether and separated by silica gel chromatography. The eluted components were dissolved in DMSO at the concentration of 100 mg mL^{-1} and filtered with a 0.22 μm filter.

2.3 MTT assay

Cells were seeded into 96-well plates at a density of 5×10^3 cells per well and incubated for 24 h before treatment with different concentrations of BRPS. Cisplatin (40 μg mL^{-1}) was used as a positive control. After treatment for 24, 48 and 72 h, 500 μg mL^{-1} MTT solution was added into each well and incubated for 3.5 h at 37 °C. The formazan products were dissolved in DMSO, and the absorbance was measured at 490 nm. The data were presented as a percentage of the control group.

2.4 Liquid chromatography-mass spectrometry (LC-MS) analysis

The samples were mixed with prechilled 80% methanol and 0.1% formic acid, and incubated on ice for 5 min, then centrifuged at 15 000*g*, 4 °C for 20 min. The supernatant was collected and diluted with LC-MS grade water to a final concentration of 53% methanol. After centrifugation at 15 000*g*, 4 °C for 20 min, the supernatant was collected and analyzed by LC-MS/MS using a Vanquish UHPLC system (Thermo Fisher, Germany) coupled with an Orbitrap Q ExactiveTMHF-X mass spectrometer (Thermo Fisher, Germany) in Novogene Co., Ltd (Beijing, China). Samples were injected into a Hypesil Gold column (100 × 2.1 mm, 1.9 μm) using a 17 min linear gradient at a flow rate of 0.2 ml min^{-1}. A Q Exactive TMHF-X mass spectrometer was operated in positive/negative polarity mode with a spray voltage of 3.2 kV, capillary temperature of 320 °C, sheath gas flow rate of 40 arb and aux gas flow rate of 10 arb.

Compound Discoverer 3.1 (CD3.1, Thermo Fisher) was used to process the raw data generated by UHPLC-MS/MS for peak alignment, peak picking, and quantitation of each metabolite, then peak intensities were normalized to the total spectral intensity. The normalized data were used to predict the molecular formula based on additive ions, molecular ion peaks and fragment ions. The peaks were matched with mzCloud (https://www.mzcloud.org/), mzVault and MassListdatabase to obtain the accurate qualitative and relative quantitative information.

2.5 Analysis of apoptosis and cell cycle

A549 cells were treated with BRPS for 24 h and stained using an AnnexinV-FITC/propidium iodide (PI) apoptosis detection kit (YEASEN, Shanghai, China) according to the manufacturer's instructions. Briefly, cells were resuspended with 1× binding buffer and Annexin V-FITC and PI were added. After incubation for 20 min in the dark at RT, stained cells were diluted with 1× binding buffer and immediately analyzed by flow cytometry.

In order to analyze the distribution of the cell cycle, cells were harvested after BRPS treatment for 24 h and fixed in cold 70% ethanol at 4 °C for 30 min. Then, cells were stained with PI (Thermo Fisher Scientific, America) for 30 min at RT. All samples were analyzed by flow cytometry.

2.6 Determination of the mitochondrial membrane potential ($\Delta\Psi_m$)

$\Delta\Psi_m$ was determined by membrane-permeable JC-1 dye (Solarbio, China). Briefly, A549 cells were treated with BRPS for 24 h, washed with PBS and stained with the JC-1 fluorescent probe according to the manufacturer's instruction for 20 min at RT. Samples were analyzed by flow cytometry and using an inverted fluorescence microscope (Nikon Eclipse Ti-E, Tokyo, Japan).

2.7 Detection of intracellular reactive oxygen species (ROS)

A549 cells were treated with BRPS for 3, 6, 12 and 24 h. After washing with PBS, the cells were stained with 10 mM fluorescent probe DCFH-DA (Solarbio, China) for 30 min at 37 °C. Samples were analyzed by flow cytometry. In some experiments, the cells were pre-treated with 5, 10 and 20 mM

N-acetyl-L-cysteine (NAC) for 1 h before the BRPS treatment to detect ROS generation.

2.8 Western blot

Proteins were extracted from the A549 cells treated with different concentrations of BRPS for 24 h and analyzed by western blot according to a previously described method.[20] Primary antibodies against GAPDH (cat. no. AG019-1), Bax (cat. no. AF1270), Bcl-2 (cat. no. AF0060), cytochrome c (cat. no. AC909-1), and cyclin B1 (cat. no. AF1606), CDK1 (cat. no. AF1516) were bought from Beyotime (China). Active caspase 3 (cat. no. E-AB-22115), cleaved PARP (cat. no. E-AB-22074), and

Table 1 Analysis of the antitumor constituents of BRPS by HPLC-MS (ESI+)

Formula	Molecular weight	RT [min]	*m/z*	Name	Tumor types	Anti-tumor activity	Ref.
$C_{12}H_{16}O_2$	192.11572	12.815	193.123	Senkyunolide A	HT-29 colon cancer	Inhibited the growth of tumor cell	23
$C_{18}H_{24}O$	256.18346	12.288	257.1908	Bakuchiol	A549 lung cancer cell	S phase arrest, caspase 9/3 activation, p53 and Bax up-regulation, Bcl-2 down-regulation	24
$C_{20}H_{26}O_4$	330.18201	11.046	353.17117	Carnosol	SGC7901 gastric cancer cells	Cell cycle arrest and apoptosis through the activation of caspases 9 and 7 and inhibition of Bcl-xL expression	25
$C_{26}H_{34}O_6$	442.23702	13.379	443.24429	Cinobufagin	U266 multiple myeloma cell	ROS-mediated activation of ERK, JNK and p38 MAPK, caspase-3 in U266 cells	26
$C_{30}H_{44}O_7$	516.3098	12.841	517.31708	Ganoderic acid A	PC-3 prostate cancer	STAT3 pathway	27
$C_{36}H_{62}O_8$	622.4453	12.914	623.45258	(20R) Ginsenoside Rh2	MCF-7, MDA-MB-231 breast cancer cells	Cell cycle arrest	28
$C_{20}H_{24}O_6$	360.15654	10.355	361.16382	Triptolide	CNE nasopharyngeal carcinoma cells	Induced Bax protein expression and inhibited phosph-NF-κB p65, Bcl-2 and VEGF proteins	29
$C_{22}H_{31}NO_3$	357.23592	11.966	358.24319	Bullatine G	SKOV3 and A2780 epithelial ovarian cancer	Anticancer effect through the GSK3β/β-catenin and Bcl-2/Bax signaling pathways	30
$C_{29}H_{44}O_8$	520.30474	14.218	521.31201	Cyasterone	A549 lung cancer cell HCT1 16 colon cancer cell	EGFR and its downstream signaling pathways	31
$C_{32}H_{46}O_8$	558.3192	11.816	559.32648	Cucurbitacin B	A549 lung cancer cell MCF-7 breast cancer cell	Induced DNA damage mediated by increasing intracellular ROS formation	32

Table 2 Analysis of the antitumor constituents of BRPS by HPLC-MS (ESI−)

Formula	Molecular weight	RT [min]	*m/z*	Name	Tumor types	Anti-tumor activity	Ref.
$C_{18}H_{30}O_2$	278.22462	13.993	277.21735	α-Linolenic acid	HT-29 colorectal cancer cell	Induced apoptosis	33
$C_{27}H_{44}O_3$	416.32924	16.657	415.32196	Calcitriol	HeLa S3 cervical cancer cell	Inhibited HeLa S3 cell proliferation, decreased HCCR-1 and increased p21 expression	34
$C_{12}H_{23}NO_{10}S_3$	437.04872	1.432	436.04144	Glucoraphanin	HepG2 hepatoma carcinoma cell	Inhibited the growth of tumor cell	35
$C_{17}H_{26}O_3$	278.18855	12.15	277.18127	6-Paradol	KB oral epidermoid carcinoma cell	Induced apoptosis through a caspase-3-dependent mechanism	36
$C_{27}H_{44}O_3$	416.32945	13.794	415.32217	Sarsasapogenin	HeLa cervical cancer	ROS-mediated mitochondrial dysfunction and ER stress cell death	37
$C_{14}H_{26}O_2$	226.19364	13.582	225.18637	Myristoleic acid	LNCaP prostate carcinoma cell	Induced apoptosis	38
$C_{35}H_{56}O_8$	604.39747	11.59	603.3902	Ziyuglycoside II	MDA-MB-231 breast cancer cells	Cell cycle arrest and cell apoptosis *via* the ROS-dependent JNK activation pathway	39
$C_{36}H_{62}O_9$	638.43977	11.168	637.4325	Ginsenoside F1	B16BL6 melanoma cell	Inhibited the growth of tumor cells	40
$C_{11}H_8O_3$	188.04774	7.303	187.04047	Plumbagin	RWPE-1 prostate cancer	Inhibited cell invasion and selectively induced apoptosis	41
$C_{24}H_{32}O_6$	416.21858	10.518	415.2113	Arenobufagin	HepG2/ADM multidrug-resistant, HepG2 hepatomacarcinoma	PI3K/Akt/mTOR pathway	42

caspase 9 (cat. no. E-AB-22035) were purchased from Elabscience (China). The HRP-conjugated secondary antibodies and ECL substrate reagents were obtained from Beyotime (China). The blots were assessed by Image J.

2.9 Library preparation for transcriptome sequencing and differential expression analysis

RNA extraction was performed with the total RNA extraction reagent (Sangon Biotech, China). RNA integrity was assessed using the RNA Nano 6000 Assay Kit of the Bioanalyzer 2100 system (Agilent Technologies, CA, USA). mRNA was purified from total RNA using poly-T oligo-attached magnetic beads for cDNA synthesis. cDNA fragments were selected and purified with the AMPure XP system (Beckman Coulter, Beverly, USA). After cluster generation, the library preparations were sequenced on an Illumina Novaseq platform and 150 bp paired-end reads were generated. Differential expression analysis of two groups was performed using the DESeq2 R package (1.20.0). Genes with an adjusted P value <0.05 found by DESeq2 were assigned a differential expression.[21]

2.10 Gene ontology (GO) and Kyoto encyclopedia of genes and genomes (KEGG) enrichment analysis of differentially expressed genes (DEGs)

GO terms with corrected P value <0.05 were considered as significant enrichment by DEGs. GO enrichment analysis and KEGG enrichment analysis of the DEGs were performed using the cluster Profiler R package.[21]

2.11 *In vivo* animal study

The right sides of female C57BL/6 mice were inoculated with 100 μL of LLC cell suspension (5×10^5 per Mouse) to establish a lung cancer mouse model. After 7 days, all mice with 15–30 mm^3 tumor were randomly divided into 6 groups (5 mice per group), which were control, DMSO, cisplatin, 100 mg kg^{-1} BRPS, 200 mg kg^{-1} BRPS and 400 mg kg^{-1} BRPS. BRPS was given every other day for 10 times and cisplatin (5 mg kg^{-1}) was injected introperitoneally every 5 days for 4 times.

Tumor sizes were measured using calipers and tumor volumes were calculated according to the following formula: tumor volume (mm^3) = (length × $width^2$)/2.

2.12 Biochemical assays

On day 28, sera were collected and the levels of aspartate aminotransferase (AST), alanine aminotransferase (ALT), urea nitrogen (BUN) and creatinine (SCR) were detected using the corresponding detection kits according to the manufacturer's protocols, respectively (Jiancheng Bioengineering Institute, China).

2.13 Analysis of immune cells in spleens of mice

On day 28, the splenocytes were separated and stained with CD3-APC/CD19-PE/CD49b-FITC, CD11b-PE/GR-1-APC, and

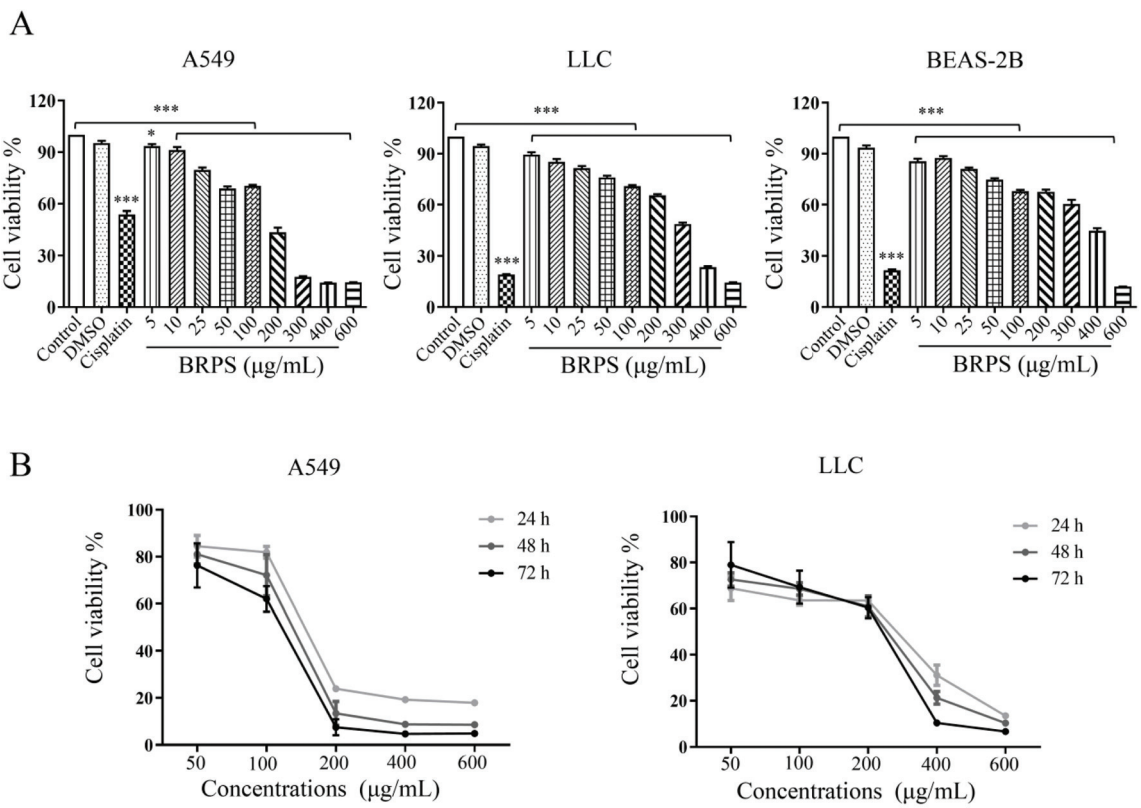

Fig. 1 Cytotoxic effect of BRPS on lung cancer cells. (A) Viability of A549, LLC and BEAS-2B cells was assessed by MTT assays. (B) BRPS inhibited the proliferation of A549 and LLC cells in a time-dependent manner. * $p < 0.05$ and *** $p < 0.001$ *vs.* control group.

CD8-APC/CD4-FITC/CD44-PE (Elabscience), and then detected by flow cytometry as previously reported.[22]

2.14 Statistical analysis

Statistical analysis was performed by one-way analysis of variance (ANOVA). The two-tailed paired *t* test was used in the inhibitors' experiments. $P < 0.05$ was considered to be statistically significant.

3 Results

3.1 Purification and identification of BRPS

On the basis of the previous studies,[19] we further optimized the extraction and separation procedure of the active components from *B. rapa*. Petroleum ether was selected to be extracted from *B. rapa*, and then the anti-lung cancer active components were separated by silica gel column chromato-

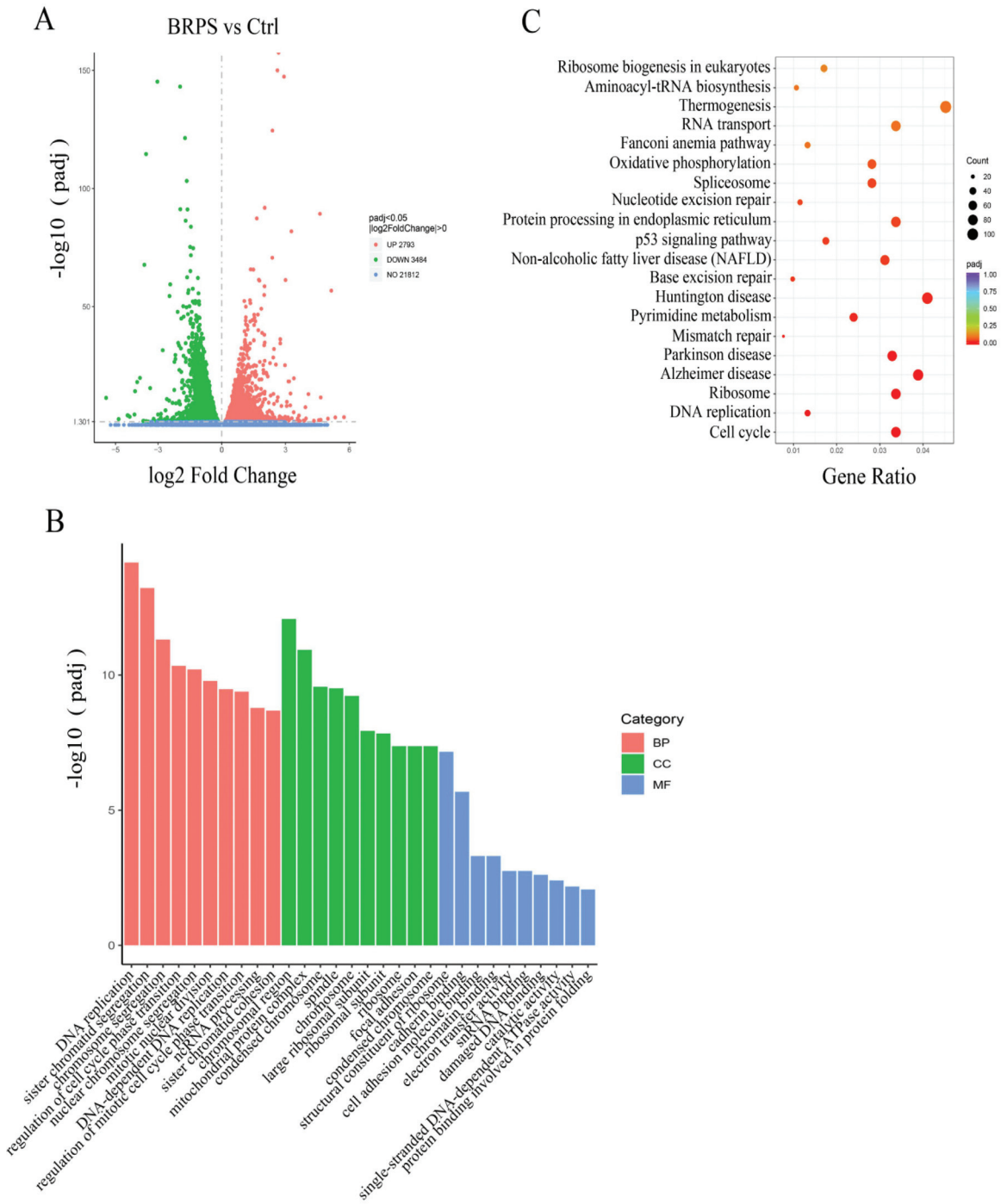

Fig. 2 Transcriptomics analysis of BRPS on A549 cells. (A) Volcano plot of BRPS *versus* control DEGs. (B) KEGG enrichment plot of BRPS *versus* control DEGs. (C) GO enrichment plot of BRPS *versus* control DEGs.

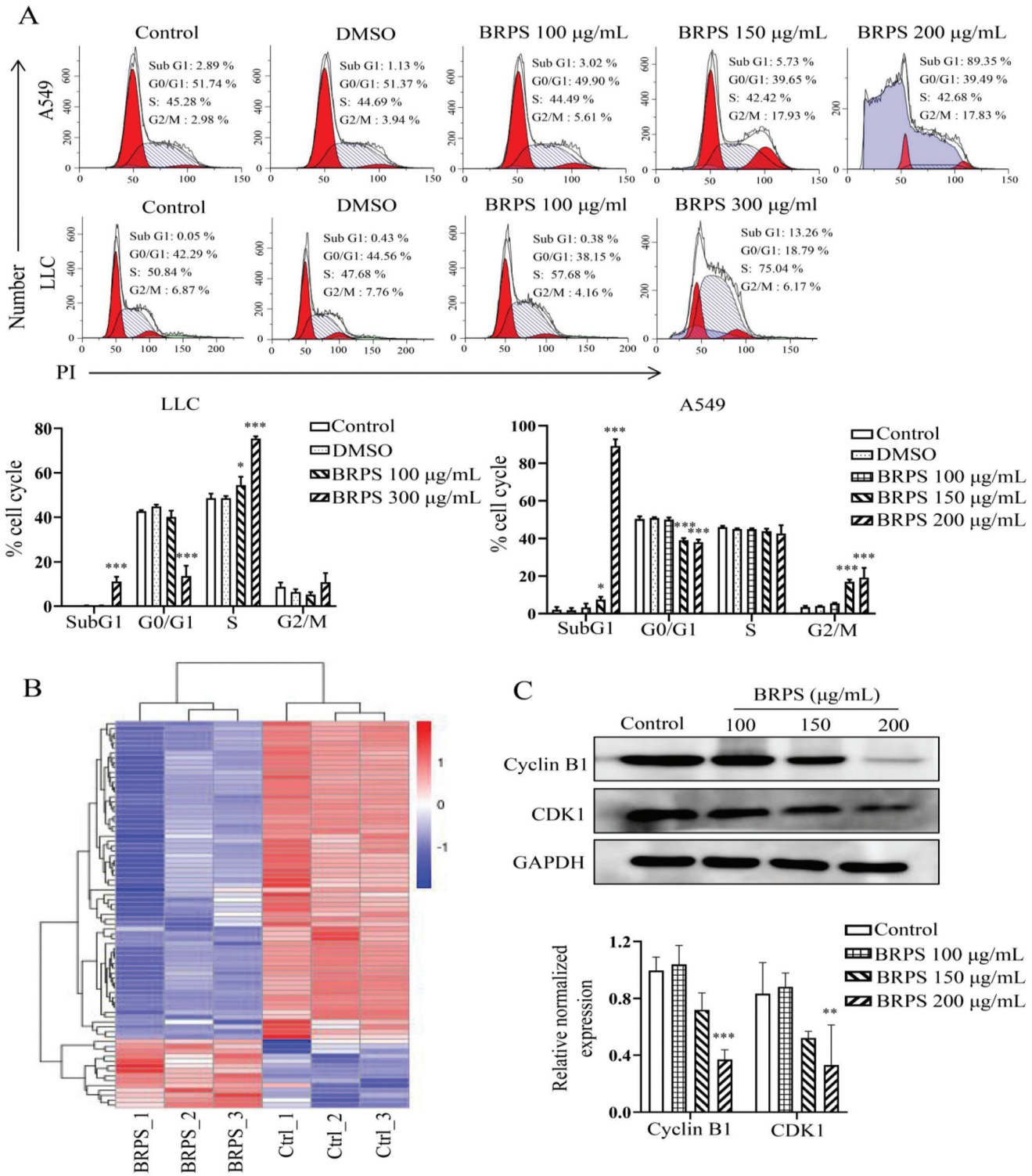

Fig. 3 Effect of BRPS on the cell cycle in A549 and LLC cells. (A) Cells were treated with different concentrations of BRPS for 24 h. After PI staining, cell cycle distribution was analyzed by flow cytometry. (B) Heat map of DEGs after treatment with BRPS for 24 h in A549 cells. (C) A549 cells were treated with different concentrations of BRPS for 24 h, and then the proteins were isolated to detect the levels of CDK1 and cyclin B1 by western blot. * $p < 0.05$, ** $p < 0.01$ and *** $p < 0.001$ *vs.* control group.

graphy and named BRPS (Fig. S1†). The components of BRPS were analyzed by LC-MS (Fig. S2†). The results show that BRPS contains lipids, lipid-like molecules, benzenoids, organic acids and derivatives, organoheterocyclic compounds and polyketides. The potential antitumor constituents of BRPS are shown in the Tables 1 and 2.

3.2 BRPS inhibited the proliferation of lung cancer cells

The antitumor activity of BRPS on A549 and LLC cells was detected by MTT assay. BRPS significantly inhibited the proliferation of A549 and LLC cells in a concentration-dependent and time-dependent manner (Fig. 1A). The IC_{50} values of BRPS

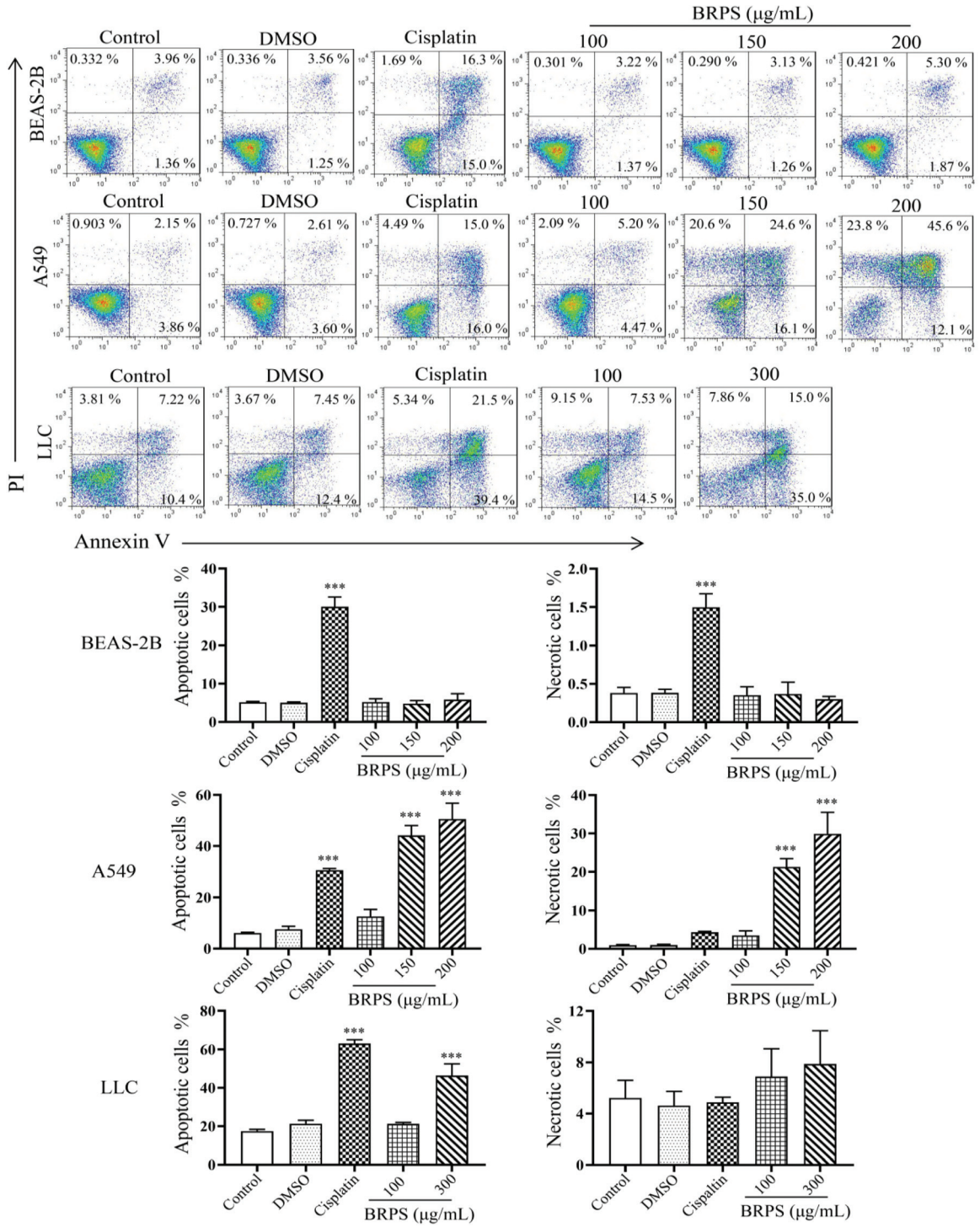

Fig. 4 Effect of BRPS on apoptosis in BEAS-2B, A549 and LLC cells. Cells were treated with different concentrations of BRPS for 24 h. The apoptosis and necrosis of A549 and BEAS-2B cells were analyzed by flow cytometry. *** $p < 0.001$ *vs.* control group.

for A549 and LLC cells were 125.1 μg mL^{-1} and 203.3 μg mL^{-1}, respectively. BEAS-2B cells were used as a normal cell control and the IC_{50} value was 263.9 μg mL^{-1} (Fig. 1B). These results suggested that BRPS might be a relatively safe drug for the treatment of lung cancer.

3.3 Potential anti-lung cancer mechanisms of BRPS

In order to clarify the anti-tumor mechanism of BRPS on A549 cells, transcriptome sequencing was performed after being treated with 150 μg mL^{-1} BRPS for 24 h. We performed differential gene analysis and screened the differentially expressed genes. Thus, a total of 6277 differentially expressed genes were detected, which were expression differential multiple $Log FC^2 > 1$ with $P < 0.05$. Thus, a total of 6277 differentially expressed genes were detected. As shown in Fig. 2A, the differences between the BRPS treatment and the control group were visualized by volcano map analysis.

All differentially expressed genes (DEGs) of A549 cells were functionally analyzed using GO and KEGG databases. Based on the GO database, DEGs were mainly concentrated and distributed in molecular functions, biological processes and cellular components. In terms of molecular function, the effects of BRPS were mainly related to the structural flow line of ribosome, electron transfer activity, damaged DNA binding, *etc*. In

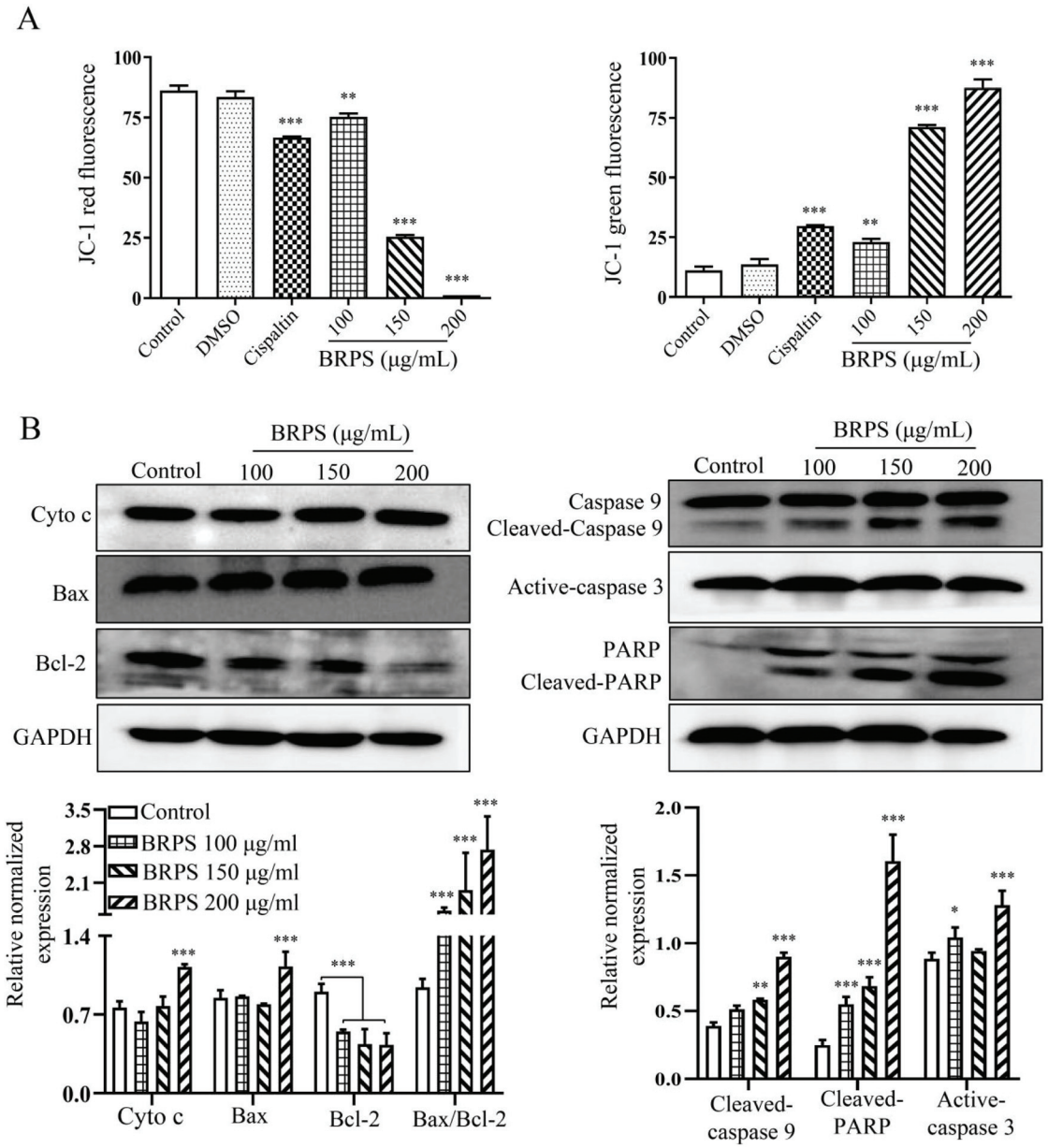

Fig. 5 Effects of BRPS on $\Delta\Psi_m$ and the caspase pathway in A549 cells. (A) A549 cells were treated with different concentrations of BRPS. After 24 h, cells were stained with JC-1 and the fluorescence changes were analyzed by flow cytometry. (B) Proteins were isolated and the levels of Bax, Bcl-2, cytochrome c, cleaved-caspases and -PARP were detected by western blot. Grayscale scanning data were obtained by Image J. * $p < 0.05$, ** $p < 0.01$ and *** $p < 0.001$ *vs.* control group.

the biological process, its effects were closely associated with DNA replication, chromosome segregation, cell cycle transition and so on. In terms of cell composition, its effects were mainly related to the chromosomal region, mitochondrial protein complex, condensed chromosome, *etc*. (Fig. 2B). The KEGG database was used to analyze the relevant anti-lung cancer pathways of BRPS. Compared with the control, the top 20 pathways including cell cycle, DNA replication and oxidative phosphorylation have been significantly changed by BRPS treatment (Fig. 2C).

3.4 BRPS induced cell cycle arrest and apoptosis in lung cancer cells

A549 and LLC cells were stained with PI after treatment with BRPS for 24 h and the cell cycle distribution was analyzed by flow cytometry. The results showed that BRPS could significantly induce cell cycle arrest at the G2/M phase in A549 cell and S phase in LLC cells (Fig. 3A). According to the KEGG enrichment analysis of 79 cell cycle-related DEGs, in which the expression of G2/M-related genes CDK1 and CyclinB1 was down-regulated (Fig. 3B). The CyclinB1 and CDK1 protein levels were also significantly downregulated by BRPS treatment in A549 cells (Fig. 3C).

In order to investigate whether the antitumor effect of BRPS on lung cancer cells was related to the induction of apoptosis, A549, LLC and BEAS-2B cells were treated with different concentrations of BRPS for 24 h. After staining with Annexin V/PI, samples were detected by flow cytometry. The results showed that BRPS significantly induced apoptosis in A549 and LLC cells, but had no effect on the apoptosis of BEAS-2B cells, suggesting that BRPS selectively induced the apoptosis of lung cancer cells in a certain range of concentration (Fig. 4).

3.5 BRPS decreased $\Delta\Psi_m$ and activated the caspase pathway in A549 cells

Reduction of $\Delta\Psi_m$ is a marker of cell apoptosis,[43] so the effect of BRPS on $\Delta\Psi_m$ of A549 cells was detected using JC-1 probe. The results showed that BRPS significantly reduced the $\Delta\Psi_m$ of A549 cells (Fig. 5A). Bcl-2 family proteins regulate the stability of the mitochondrial structure and function.[44] As shown in Fig. 5B, BRPS significantly increased the protein level of pro-apoptotic factor Bax and decreased the protein level of anti-

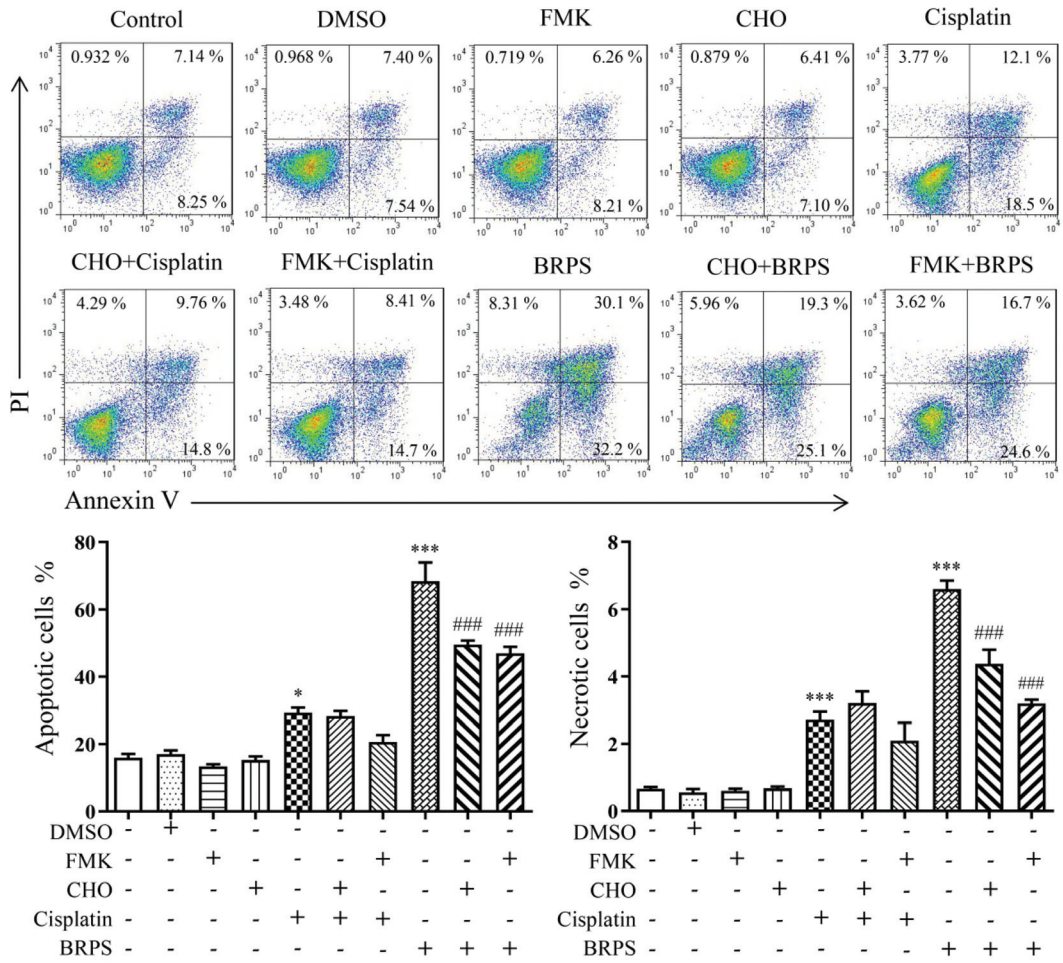

Fig. 6 Effects of caspase inhibitors on the BRPS-induced apoptosis of A549 cells. * $p < 0.05$ and *** $p < 0.001$ *vs.* control group, ### $p < 0.001$ *vs.* BRPS treatment group.

apoptotic factor Bcl-2. The increased ratio of Bax/Bcl-2 caused the reduction of $\Delta\Psi_m$, which could promote the release of cytochrome c.[45] Western blot results showed that BRPS significantly increased the release of cytochrome c in A549 cells. The release of cytochrome c activates the caspase cascade pathway and induces apoptosis.[46] Subsequently, the levels of activated caspase 9 and caspase 3 were up-regulated by BRPS treatment after 24 h, which led to the cleavage of PARP.

To further confirm the role of the caspase pathway in BRPS-induced apoptosis, A549 cells were pretreated with caspase inhibitor Z-VAD-FMK (FMK) and caspase 3 inhibitor Ac-DEVD-CHO (CHO) for 2 h, and then treated with 150 μg mL^{-1} BRPS for 24 h to detect A549 cell apoptosis by flow cytometry. The results showed that FMK and CHO significantly inhibited the BRPS-induced apoptosis of A549 cells (Fig. 6). These results suggested that BRPS induced A549 cell apoptosis through the mitochondria-dependent pathway.

3.6 BRPS increased ROS in A549 cells

ROS play an important role in cell apoptosis.[47] A549 cells were treated with different concentrations of BRPS for 3, 6, 12 and 24 h. After staining with DCFH-DA, samples were analyzed by flow cytometry. As shown in Fig. 7A, BRPS significantly increased the levels of ROS in A549 cells in a dose-and time-dependent manner. ROS inhibitor NAC (*N*-acetyl-L-cysteine) pretreatment significantly inhibited ROS and apoptosis in

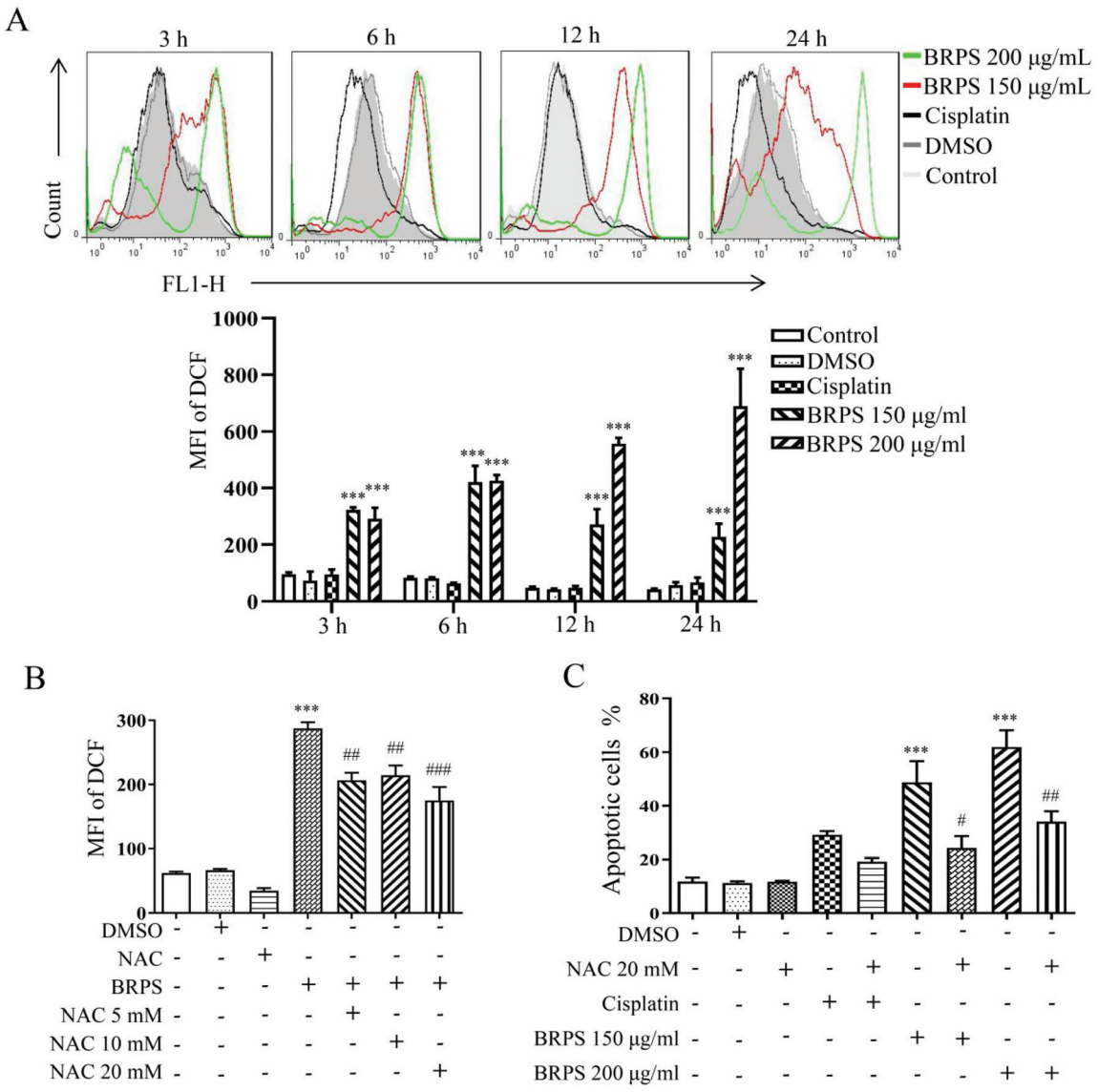

Fig. 7 Effects of BRPS on ROS in A549 cells. (A) A549 cells were treated with different concentrations of BRPS for 3, 6, 12 and 24 h, respectively. After staining with DCFH-DA, cells were analyzed by flow cytometry. A549 cells were subjected to BRPS treatment after being pretreated with NAC for 1 h, (B) the levels of ROS were detected, (C) and the apoptosis of A549 cells was analyzed by flow cytometry. *** $p < 0.001$ *vs.* control group, ## $p < 0.01$ and ### $p < 0.001$ *vs.* BRPS treatment group.

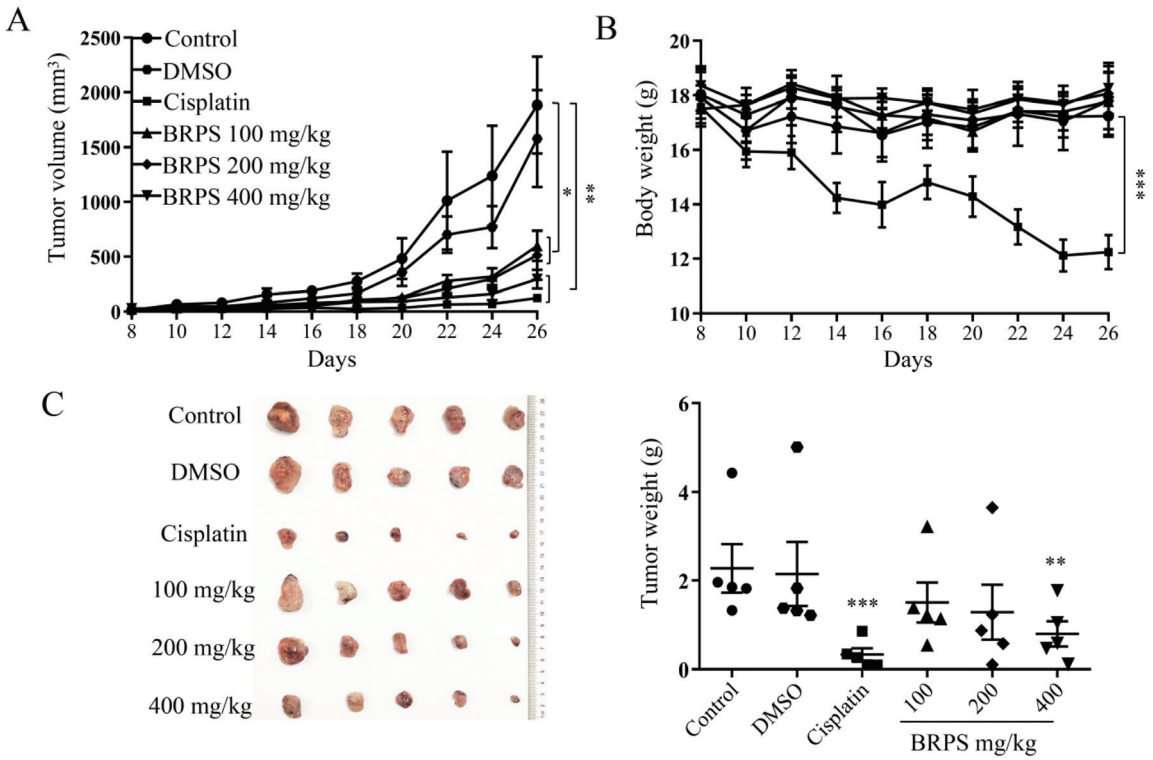

Fig. 8 Anti-tumor effects of BRPS *in vivo*. 5 × 10^5 LLC cells were injected to the right side and mice were randomly divided into six groups when the tumors reached a size of approximately 15–30 mm^3 in all mice. (A) Tumor volumes were assessed every other day during drug treatment. (B) Body weight was assessed every other day during drug treatment. (C) Tumors were weighted after sacrificed.* $p < 0.05$, ** $p < 0.01$ and *** $p < 0.001$ *vs.* control group.

A549 cells induced by BRPS (Fig. 7B and C). These results indicated that the inhibitory effect of BRPS on A549 cells might depend on the production of ROS.

3.7 BRPS suppressed lung cancer cell growth *in vivo*

In order to verify whether BRPS can suppress the growth of lung cancer cells *in vivo*, we established a LLC tumor mouse model. From the 8th day, ten BRPS and three cisplatin treatments were injected intraperitoneally. Compared to the control group, BRPS and cisplatin groups significantly suppressed tumor cell growth (Fig. 8A). Notably, there was no change in body weight in the BRPS groups, but a significant decrease of body weight was observed in the cisplatin group (Fig. 8B).

On day 28, the mice were sacrificed, and the tumor tissues and organs were isolated and weighed, and the photograph of tumors was taken and is shown in Fig. 8C. The tumor weight was significantly decreased in the cisplatin and high-dose BRPS groups. The organ indexes were calculated and there was no significant change in organ indexes among all groups except the spleen indexes, which were significantly decreased in the cisplatin group compared with the control group, indicating that cisplatin had severe side effects on mice (Fig. 9A). Next, HE staining was performed on tumor, liver and kidney tissues. As shown in Fig. 9B, compared with the control group, the tumor tissues of the BRPS treated group had significantly fewer nuclei and appeared to have necrotic areas and there were no pathological changes in liver and kidney tissues among all groups. Blood biochemical examination was further carried out to evaluate the function of liver and kidneys, which included alanine aminotransferase (ALT), aspartate aminotransferase (AST), urea nitrogen (BUN) and creatinine (Cr). We observed that BRPS reduced the levels of ALT and BUN in blood, indicating a certain protective effect (Fig. 9C). The results suggested that BRPS significantly inhibited the growth of lung cancer cells *in vivo* without side effects.

3.8 BRPS enhanced the immunity of tumor-bearing mice

To investigate whether the antitumor effect of BRPS *in vivo* is related to immunity, the proportions of immune cells in spleens of tumor-bearing mice was detected by flow cytometry. Compared with the control group, the proportions of B cells, $CD4^+$ T cells, $CD8^+$ T cells and activated $CD8^+$ T cells ($CD44^+$) were significantly increased in the BRPS group (Fig. 10A, C and D), while the proportions of NK cells and activated $CD4^+$ T cells ($CD44^+$) were not significantly changed (Fig. 10B). Moreover, the proportions of myeloid-derived suppressor cells ($CD11b^+Gr\text{-}1^+$) in the high-dose BRPS group were decreased to some extent (Fig. 10E). These results suggested that BRPS enhanced the immunity of tumor-bearing mice.

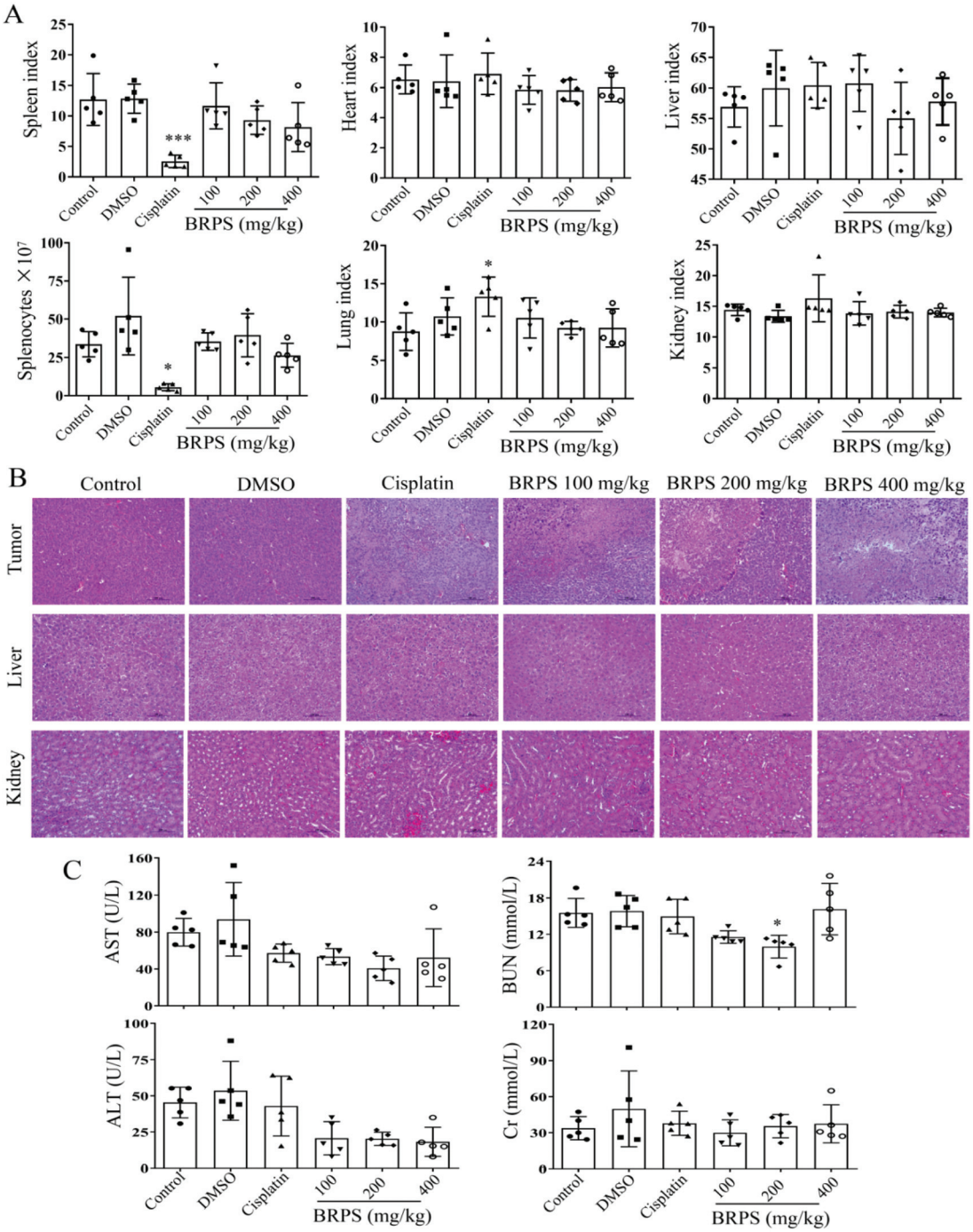

Fig. 9 Effects of BRPS on organ indexes, liver and kidney function and histological morphology in mice. (A) On day 28, all organs were isolated and the organ indexes were calculated. (B) The tumors, livers and kidneys were pathologically evaluated. (C) The indexes related to liver and kidney function were calculated. * $p < 0.05$ *vs.* control group.

4 Discussion

The occurrence and development of lung cancer are related to multiple genes and signaling pathways. Lung cancer is difficult to cure with a high mortality rate.[48] Screening anti-tumor drugs from natural products has become a research hotspot.[49]

In this study, we found that BRPS significantly inhibited the growth of A549 and LLC cells through induction of cell cycle arrest and apoptosis. The key of carcinogenesis is the uncontrolled proliferation of tumor cells due to the disorder of cell cycle regulation. The induction of cell cycle arrest and apoptosis may be the main strategies for the prevention and treatment of cancer.[50] Our transcriptome analysis showed that

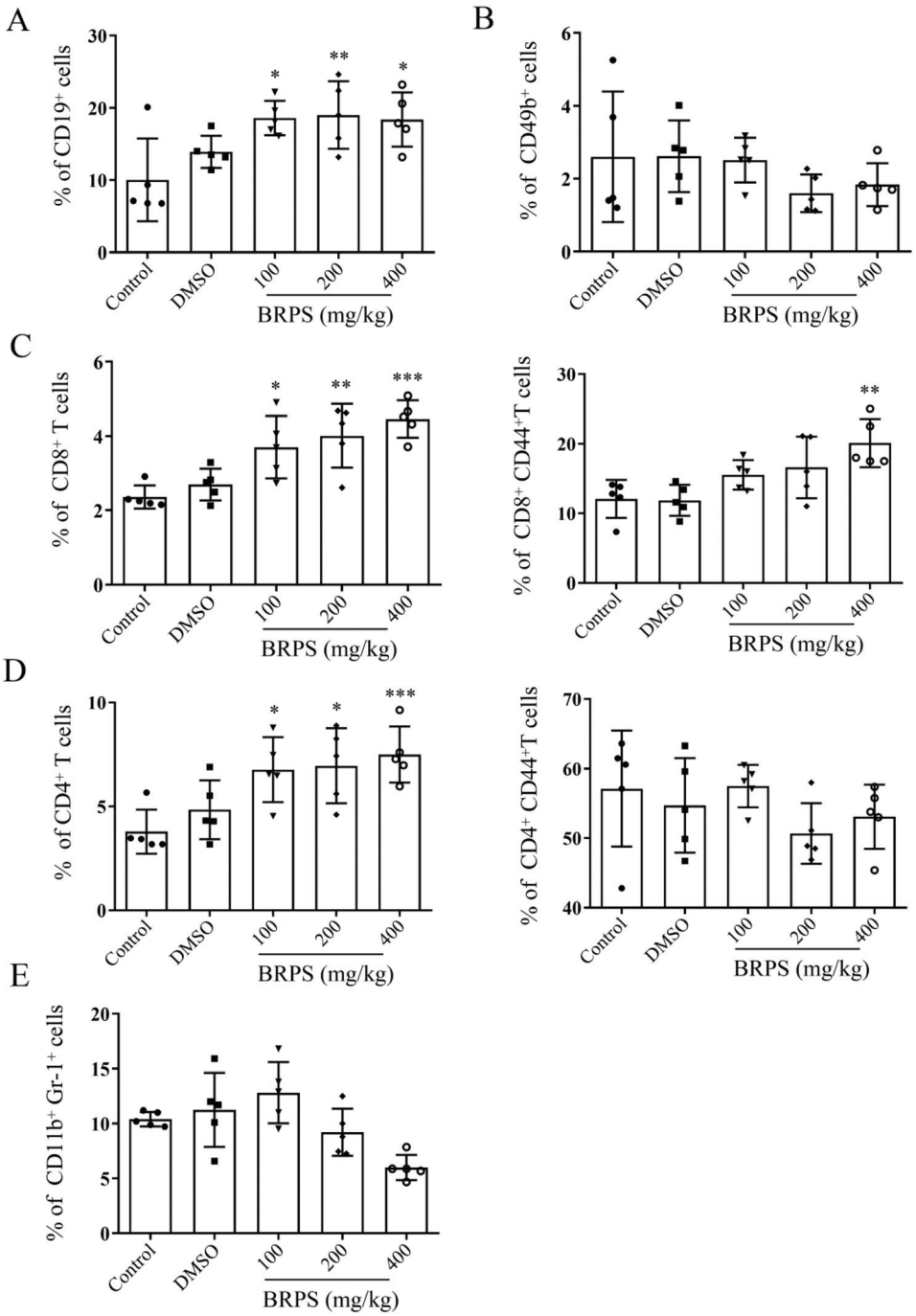

Fig. 10 The percentages of B cells, NK cells, $CD4^+$ and $CD8^+$ T cells and MDSC after treatment with BRPS. Splenocytes were isolated 28 days after treatment with BRPS. The freshly isolated splenocytes were used to analyze the percentages of B cells (A), NK cells (B), $CD4^+$, $CD44^+CD4^+$ T cells (C), $CD8^+$, $CD44^+CD8^+$T cells (D) and MDSCs (E). * $p < 0.05$, ** $p < 0.01$ and *** $p < 0.001$ *vs.* control group.

DEGs induced by BRPS were enriched in the cell cycle and DNA replication. The binding of CDK1 and its regulatory subunit cyclin B1 can activate the cyclin B1/CDK1 complex, which is responsible for the transition from the G2 to M phase.[51] In this study, the levels of cyclin B1 and CDK1 were greatly decreased by BRPS treatment in a dose-dependent manner. This is consistent with the cell cycle arrest at the G2/M phase induced by BRPS. These results suggested that the inhibitory effect of BRPS on the growth of A549 cells was related to the induction of cell cycle arrest.

Apoptosis is a process of programmed cell death characterized by a variety of biochemical and morphological changes including cell shrinkage, chromatin condensation, and DNA fragmentation.[52] Apoptosis and cell cycle disorder are closely

related events, and the disruption of cell cycle process may eventually lead to apoptosis or necrosis.[53] Here, we observed that BRPS dose-dependently induced apoptosis in A549 cells.

Apoptosis can be initiated by either the death receptor pathway or mitochondria-dependent pathway. The Bcl-2 family proteins are known as key regulators of apoptosis including anti-apoptotic members (Bcl-2 and Bcl-xL) and pro-apoptotic members (Bax and Bad). An elevated Bax/Bcl-2 ratio causes a release of cytochrome c from mitochondria to the cytosol where it activates caspase-9. Subsequently, the active caspase-9 can activate caspase-3, which cleaves PARP at the onset of apoptosis.[54] In this study, BRPS greatly increased the Bax/Bcl-2 ratio that caused the decrease of $\Delta\Psi_m$ in A549 cells, then the release of cytochrome c was up-regulated, following the activation of caspase 9 and caspase 3. Finally, PARP was cleaved by active caspase 3. Moreover, the BRPS-induced apoptosis could be partially attenuated by the caspase 3 inhibitor Ac-DEVD-CHO and the caspase inhibitor Z-VAD-FMK. These results suggested that BRPS induced lung cancer cell apoptosis by activating the mitochondrial apoptosis pathway.

ROS, as a second messenger in a variety of signaling pathways, plays an important role in apoptosis by regulating the activity of certain enzymes in cell death pathways.[55,56] In this study, we found that BRPS treatment significantly increased ROS levels in A549 cells. NAC pretreatment partially reduced the generation of ROS of A549 cells induced by BRPS. Interestingly, ziyuglycoside II, a compound in BRPS, induced apoptosis in breast cancer cells by regulating ROS and JNK signaling pathways.[39]

In a lung cancer mouse model, BRPS significantly inhibited the growth of LLC cells without liver and kidney damage and obvious side effects. Cisplatin also significantly inhibited tumor growth, but the body weight and spleen indexes of mice in this group decreased significantly, which might be related to its side effects. Chinese herbal medicine plays an antitumor role by inhibiting tumor progression and improving the body's immune system. More and more pieces of evidence show that many TCMs have good immunomodulatory effects.[57,58] Our study showed that BRPS treatment increased the proportions of B cells, $CD4^+$ T cells, $CD8^+$ T cells, and activated $CD8^+$ T cells in the spleens of tumor-bearing mice. These results suggest that BRPS have certain immune-enhancing activities.

TCM can be used as adjuvant therapy and is currently applied in clinical practice in combination with chemotherapy for the treatment of lung cancer, thus reducing the toxic side effects of chemotherapy for lung cancer patients, improving the quality of life of patients and increasing the survival rate of lung cancer patients.[59–61] *B. rapa* is widely distributed in Xinjiang, China, and BRPS obtained by isolation from *B. rapa* has the characteristics of a simple preparation method and easy access. In this study, BRPS not only inhibited the growth of lung cancer cells *in vivo* but also enhanced the immunity of mice and is expected to be a combination therapy drug for lung cancer.

5 Conclusion

In conclusion, BRPS inhibited the growth of lung cancer cells *in vitro* by inducing cell cycle arrest and mitochondria-dependent apoptosis and suppressed lung cancer growth *in vivo* through a direct antitumor effect and indirect immune-enhancing activities. BRPS might be used as a potential candidate for the treatment of lung cancer.

Ethnics statement

The experimental protocol was approved by the Committee on the Ethics of Animal Experiments of Xinjiang Key Laboratory of Biological Resources and Genetic Engineering (BRGE-AE001).

Author contributions

Xierenguli Halike, Jinyu Li, Pengfei Yuan, Kaimeiliya yasheng, Min Chen performed experiments, analyzed data and prepared figures. Jinyao Li and Lijie Xia designed the experiments and wrote the paper. All authors reviewed the manuscript.

Conflicts of interest

The authors declared no potential conflicts of interest with respect to the research, authorship, and/or publication of this article.

Acknowledgements

This work was supported by the Natural Science Foundation of Xinjiang Uyghur Autonomous Region, China (2021D01A119), the National Natural Science Foundation of China (31860258), and the Doctoral Start-up Foundation of Xinjiang University (BS180222).

References

1 H. Sung, J. Ferlay, R. L. Siegel, M. Laversanne, I. Soerjomataram, A. Jemal and F. Bray, Global cancer statistics 2020: GLOBOCAN estimates of incidence and mortality worldwide for 36 cancers in 185 countries, *Ca-Cancer J. Clin.*, 2021, 1–41.
2 S. Wei, H. Zhang and S. Tao, A review of arsenic exposure and lung cancer, *Toxicol. Res.*, 2019, **8**, 319–327.
3 C. Soza-Ried, E. Bustamante, C. Caglevic, C. Rolfo, R. Sirera and H. Marsiglia, Oncogenic role of arsenic exposure in lung cancer: A forgotten risk factor, *Crit. Rev. Oncol. Hematol.*, 2019, **139**, 128–133.

4 B. C. Bade and C. S. Dela Cruz, Lung Cancer 2020: Epidemiology, Etiology, and Prevention, *Clin. Chest Med.*, 2020, **41**, 1–24.
5 M. Sánchez-Céspedes, Lung cancer biology: A genetic and genomic perspectiv, *Clin. Transl. Oncol.*, 2009, **11**, 263–269.
6 A. Manerikar, M. Querrey, E. Cerier, S. Kim, D. D. Odell, L. L. Pesce and A. Bharat, Comparative Effectiveness of Surgical Approaches for Lung Cance, *J. Surg. Res.*, 2020, 1–11.
7 S. K. Vinod and E. Hau, Radiotherapy treatment for lung cancer: Current status and future directions, *Respirology*, 2020, **25**, 61–71.
8 R. Pirker, Chemotherapy remains a cornerstone in the treatment of nonsmall cell lung cancer, *Curr. Opin. Oncol.*, 2020, **32**, 63–67.
9 R. Ruiz-Cordero and W. P. Devine, Targeted Therapy and Checkpoint Immunotherapy in Lung Cancer, *Surg. Pathol. Clin.*, 2020, **13**, 17–33.
10 Z. Li, Z. Feiyue and L. Gaofeng, Traditional Chinese medicine and lung cancer——From theory to practice, *Biomed. Pharmacother.*, 2021, **137**, 111381.
11 A. Rw, B. B. Jie, L. C. Zhan, Z. A. Kai and A. Ht, Biological activity of Brassica rapa L. polysaccharides on RAW264.7 macrophages and on tumor cells, *Bioorg. Med. Chem.*, 2020, **28**, 115330.
12 M. Francisco, D. A. Moreno, M. E. Cartea, F. Ferreres, C. García-Viguera and P. Velasco, Simultaneous identification of glucosinolates and phenolic compounds in a representative collection of vegetable Brassica rapa, *J. Chromatogr. A*, 2009, **1216**, 6611–6619.
13 A. Romani, P. Vignolini, L. Isolani, F. Ieri and D. Heimler, HPLC-DAD/MS characterization of flavonoids and hydroxycinnamic derivatives in turnip tops (Brassica rapa L. Subsp. sylvestris L.), *J. Agric. Food Chem.*, 2006, **54**, 1342–1346.
14 Z. E. Chen, R. Wufuer, J. H. Ji, J. F. Li, Y. F. Cheng, C. Dong and H. Taoerdahong, Structural characterization and immunostimulatory activity of polysaccharides from Brassica rapa L., *J. Agric. Food Chem.*, 2017, **65**, 9685–9692.
15 Q. Wu, J. G. Cho, D. S. Lee, D. Y. Lee, N. Y. Song, Y. C. Kim, K. T. Lee, H. G. Chung, M. S. Choi, T. S. Jeong, E. M. Ahn, G. S. Kim and N. I. Baek, Carbohydrate derivatives from the roots of Brassica rapa ssp. campestris and their effects on ROS production and glutamate-induced cell death in HT-22 cells, *Carbohydr. Res.*, 2013, **372**, 9–14.
16 K. Yamamoto, K. Furuya, K. Yamada, F. Takahashi, C. Hamajima and S. Tanaka, Enhancement of natural killer activity and IFN-γ production in an IL-12-dependent manner by a Brassica rapa L., *Biosci., Biotechnol., Biochem.*, 2017, **82**, 1–15.
17 Y. Xie, S. Jiang, D. Su, N. Pi, C. Ma and P. Gao, Composition analysis and anti-hypoxia activity of polysaccharide from Brassica rapa L., *Int. J. Biol. Macromol.*, 2010, **47**, 528–533.
18 G. U. Seong, I. W. Hwang and S. K. Chung, Antioxidant capacities and polyphenolics of Chinese cabbage (Brassica rapa L. ssp. Pekinensis) leaves, *Food Chem.*, 2016, **199**, 612–618.
19 A. Aipire, Q. Chen, S. Cai, J. Li, C. Fu, T. Ying, J. Lu and J. Li, N-butanol subfraction of Brassica Rapa L. promotes reactive oxygen species production and induces apoptosis of A549 lung adenocarcinoma cells via mitochondria-dependent pathway, *Molecules*, 2018, **23**, 1–12.
20 Y. Yang, P. Yuan, X. Wei, C. Fu, J. Li, W. Wang, X. Wang, Y. Li and J. Li, Cultivated and wild Pleurotus ferulae ethanol extracts inhibit hepatocellular carcinoma cell growth via inducing endoplasmic reticulum stress- and mitochondria-dependent apoptosis, *Sci. Rep.*, 2018, **8**, 13984.
21 Y. Chen, L. Si, J. Zhang, H. Yu and Y. Wu, Uncovering the Antitumor Effects and Mechanisms of Shikonin Against Colon Cancer on Comprehensive Analysis, *Phytomedicine*, 2021, **82**, 153460.
22 J. Li, J. Li, A. Aipire, J. J. Luo, P. Yuan and F. Zhang, The combination of Pleurotus ferulae water extract and CpG-ODN enhances the immune responses and antitumor efficacy of HPV peptides pulsed dendritic cell-based vaccine, *Vaccine*, 2016, **34**, 3568–3575.
23 W. L. T. Kan, C. H. Cho, J. A. Rudd and G. Lin, Study of the anti-proliferative effects and synergy of phthalides from Angelica sinensis on colon cancer cells, *J. Ethnopharmacol.*, 2008, **120**, 36–43.
24 Z. Chen, K. Jin, L. Gao, G. Lou, Y. Jin, Y. Yu and Y. Lou, Anti-tumor effects of bakuchiol, an analogue of resveratrol, on human lung adenocarcinoma A549 cell line, *Eur. J. Pharmacol.*, 2010, **643**, 170–179.
25 L. Wang, Y. Zhang, K. Liu, H. Chen, R. Yang, X. Ma, H. G. Kim, A. M. Bode, D. J. Kim and Z. Dong, Carnosol suppresses patient-derived gastric tumor growth by targeting RSK2, *Oncotarget*, 2018, **9**, 34200–34212.
26 S. H. Baek, C. Kim, J. H. Lee, D. Nam, J. Lee, S. G. Lee, W. S. Chung, H. J. Jang, S. H. Kim and K. S. Ahn, Cinobufagin exerts anti-proliferative and pro-apoptotic effects through the modulation ROS-mediated MAPKs signaling pathway, *Immunopharmacol. Immunotoxicol.*, 2015, **37**, 265–273.
27 B. S. Gill, S. Kumar and Navgeet, Evaluating anti-oxidant potential of ganoderic acid A in STAT 3 pathway in prostate cancer, *Mol. Biol. Rep.*, 2016, **43**, 1411–1422.
28 S. Choi, T. W. Kim and S. V. Singh, Ginsenoside Rh2-mediated G1 phase cell cycle arrest in human breast cancer cells is caused by p15 Ink4B and p27 Kip1 -dependent Inhibition of Cyclin-dependent Kinases, *Pharm. Res.*, 2009, **26**, 2280–2288.
29 W. Zhang, M. Kang, T. Zhang, B. Li, X. Liao and R. Wang, Triptolide combined with radiotherapy for the treatment of nasopharyngeal carcinoma via NF-κB-related mechanism, *Int. J. Mol. Sci.*, 2016, **17**, 2139.
30 H. Zhang, R. Dong, P. Zhang and Y. Wang, Songorine suppresses cell growth and metastasis in epithelial ovarian cancer via the Bcl–2/Bax and GSK3β/β–catenin signaling pathways, *Oncol. Rep.*, 2019, **41**, 3069–3079.

31 X. G. Lu, H. F. Qiu, L. Yang, J. Y. Zhang, S. J. Ma and L. Zhen, Anti-proliferation effects, efficacy of cyasterone in vitro and in vivo and its mechanism, *Biomed. Pharmacother.*, 2016, **84**, 330–339.

32 J. Guo, G. Wu, J. Bao, W. Hao, J. Lu and X. Chen, Cucurbitacin B induced ATM-mediated DNA damage causes G2/M cell cycle arrest in a ROS-dependent manner, *PLoS One*, 2014, **9**, e88140.

33 M. J. González-Fernández, I. Ortea and J. L. Guil-Guerrero, α-Linolenic and γ-linolenic acids exercise differential anti-tumor effects on HT-29 human colorectal cancer cells, *Toxicol. Res.*, 2020, **9**, 474–483.

34 G. Wang, L. Lei, X. Zhao, J. Zhang, M. Zhou and K. Nan, Calcitriol inhibits cervical cancer cell proliferation through downregulation of HCCR1 expression, *Oncol. Res.*, 2015, **22**, 301–309.

35 A. F. Abdull Razis and N. M. Noor, Sulforaphane is Superior to Glucoraphanin in Modulating Carcinogen-Metabolising Enzymes in Hep G2 Cells, *Asian Pac. J. Cancer Prev.*, 2013, **14**, 4235–4238.

36 Y. S. Keum, J. Kim, K. H. Lee, K. K. Park, Y. J. Surh, J. M. Lee, S. S. Lee, J. H. Yoon, S. Y. Joo, I. H. Cha and J. I. Yook, Induction of apoptosis and caspase-3 activation by chemopreventive [6]-paradol and structurally related compounds in KB cells, *Cancer Lett.*, 2002, **177**, 41–47.

37 S. Shen, Y. Zhang, R. Zhang and X. Gong, Sarsasapogenin induces apoptosis via the reactive oxygen species-mediated mitochondrial pathway and ER stress pathway in HeLa cells, *Biochem. Biophys. Res. Commun.*, 2013, **441**, 519–524.

38 K. Iguchi, N. Okumura, S. Usui, H. Sajiki, K. Hirota and K. Hirano, Myristoleic acid, a cytotoxic component in the extract from Serenoa repens, induces apoptosis and necrosis in human prostatic LNCaP cells, *Prostate*, 2001, **47**, 59–65.

39 X. Zhu, K. Wang, K. Zhang, L. Zhu and F. Zhou, Ziyuglycoside II induces cell cycle arrest and apoptosis through activation of ROS/JNK pathway in human breast cancer cells, *Toxicol. Lett.*, 2014, **227**, 65–73.

40 D. D. Wang, Y. Jin, C. Wang, Y. J. Kim, Z. E. J. Perez, N. I. Baek, R. Mathiyalagan, J. Markus and D. C. Yang, Rare ginsenoside Ia synthesized from F1 by cloning and over-expression of the UDP-glycosyltransferase gene from Bacillus subtilis: synthesis, characterization, and in vitro melanogenesis inhibition activity in BL6B16 cells, *J. Ginseng Res.*, 2018, **42**, 42–49.

41 M. H. Aziz, N. E. Dreckschmidt and A. K. Verma, Plumbagin, a medicinal plant-derived naphthoquinone, is a novel inhibitor of the growth and invasion of hormone-refractory prostate cancer, *Cancer Res.*, 2008, **68**, 9024–9032.

42 D. M. Zhang, J. S. Liu, L. J. Deng, M. F. Chen, A. Yiu, H. H. Cao, H. Y. Tian, K. P. Fung, H. Kurihara, J. X. Pan and W. C. Ye, Arenobufagin, a natural bufadienolide from toad venom, induces apoptosis and autophagy in human hepatocellular carcinoma cells through inhibition of PI3K/Akt/mTOR pathway, *Carcinogenesis*, 2013, **34**, 1331–1342.

43 Y. Zhao, J. Liu and L. Liu, Artesunate inhibits lung cancer cells via regulation of mitochondrial membrane potential and induction of apoptosis, *Mol. Med. Rep.*, 2020, **22**, 3017–3022.

44 N. Popgeorgiev, J. Sa, L. Jabbour, S. Banjara and M. Kvansakul, Ancient and conserved functional interplay between Bcl-2 family proteins in the mitochondrial pathway of apoptosis, *Sci. Adv.*, 2020, **6**, eabc4149.

45 E. Gottlieb, S. M. Armour, M. H. Harris and C. B. Thompson, Mitochondrial membrane potential regulates matrix configuration and cytochrome c release during apoptosis, *Cell Death Differ.*, 2003, **10**, 709–717.

46 C. A. Elena-Real, A. Díaz-Quintana, K. González-Arzola, A. Velázquez-Campoy, M. Orzáez, A. López-Rivas, S. Gil-Caballero, M. Á. De la Rosa and I. Díaz-Moreno, Cytochrome c speeds up caspase cascade activation by blocking 14-3-3ε-dependent Apaf-1 inhibition, *Cell Death Dis.*, 2018, **9**, 365.

47 B. Perillo, M. Di Donato, A. Pezone, E. Di Zazzo, P. Giovannelli, G. Galasso, G. Castoria and A. Migliaccio, ROS in cancer therapy: the bright side of the moon, *Exp. Mol. Med.*, 2020, **52**, 192–203.

48 J. W. Clark and D. L. Longo, Recent progress in systemic treatment for lung cancer, *Curr. Opin. Pulm. Med.*, 2018, **24**, 355–366.

49 Y. J. Lin, W. M. Liang, C. J. Chen, H. Tsang, J. S. Chiou, X. Liu, C. F. Cheng, T. H. Lin, C. C. Liao, S. M. Huang, J. Chen, F. J. Tsai and T. M. Li, Network analysis and mechanisms of action of Chinese herb-related natural compounds in lung cancer cells, *Phytomedicine*, 2019, **58**, 152893.

50 K. Vermeulen, Z. N. Berneman and D. R. Van Bockstaele, Cell cycle and apoptosis, *Cell Proliferation*, 2003, **36**, 165–175.

51 M. Malumbres and M. Barbacid, Cell cycle, CDKs and cancer: A changing paradigm, *Nat. Rev. Cancer*, 2009, **9**, 153–166.

52 J. Barman, R. Kumar, G. Saha, K. Tiwari and V. K. Dubey, Apoptosis: Mediator Molecules, Interplay with Other Cell Death Processes and Therapeutic Potentials, *Curr. Pharm. Biotechnol.*, 2018, **19**, 644–663.

53 G. I. Evan and K. H. Vousden, Proliferation, cell cycle and apoptosis in cancer, *Nature*, 2001, **411**, 342–348.

54 Y. Deng, X. Li, X. Li, Z. Zheng, W. Huang, L. Chen, Q. Tong and Y. Ming, Corilagin induces the apoptosis of hepatocellular carcinoma cells through the mitochondrial apoptotic and death receptor pathways, *Oncol. Rep.*, 2018, **39**, 2545–2552.

55 J. N. Moloney and T. G. Cotter, ROS signalling in the biology of cancer, *Semin. Cell Dev. Biol.*, 2018, **80**, 50–64.

56 Y. Wang, J. Zhang, Y. Yang, Q. Liu, G. Xu, R. Zhang and Q. Pang, ROS generation and autophagosome accumulation contribute to the DMAMCL-induced inhibition of glioma cell proliferation by regulating the ROS/MAPK signaling pathway and suppressing the Akt/mTOR signaling pathway, *OncoTargets Ther.*, 2019, **12**, 1867–1880.

57 H. Fu, L. Jin, X. Shao, Y. Li, F. Chen, Z. Shou, X. Tang, B. Ji and Q. Shou, Hirsutella sinensis Inhibits Lewis Lung Cancer via Tumor Microenvironment Effector T Cells in Mice, *Am. J. Chin. Med.*, 2018, **46**, 911–922.

58 S. Wang, S. Long, Z. Deng and W. Wu, Positive Role of Chinese Herbal Medicine in Cancer Immune Regulation, *Am. J. Chin. Med.*, 2020, **48**, 1577–1592.

59 Y. H. Liao, C. I. Li, C. C. Lin, J. G. Lin, J. H. Chiang and T. C. Li, Traditional Chinese medicine as adjunctive therapy improves the long-term survival of lung cancer patients, *J. Cancer Res. Clin. Oncol.*, 2017, **143**, 2425–2435.

60 X. Zhao, X. Dai, S. Wang, T. Yang, Y. Yan, G. Zhu, J. Feng, B. Pan, M. Sunagawa, X. Zhang, Y. Qian and Y. Liu, Traditional Chinese Medicine Integrated with Chemotherapy for Stage II-IIIA Patients with Non-Small-Cell Lung Cancer after Radical Surgery: A Retrospective Clinical Analysis with Small Sample Size, *Evid. Based Complement. Alternat. Med.*, 2018, **2018**, 4369027.

61 M. Y. Huang, L. L. Zhang, J. Ding and J. J. Lu, Anticancer drug discovery from Chinese medicinal herbs, *Chin. Med.*, 2018, **13**, 35.